



Autonomous Damage Source Monitoring in Composite Structures

Shirsendu Sikdar, Rakesh Mishra and Karl Walton

EasyChair preprints are intended for rapid dissemination of research results and are integrated with the rest of EasyChair.

December 5, 2023

Autonomous Damage Source Monitoring in Composite Structures

¹Shirsendu Sikdar
School of Computing and Engineering
United Kingdom
University of Huddersfield
Huddersfield, United Kingdom
<https://orcid.org/0000-0001-6897-0247>

²Rakesh Mishra
School of Computing and Engineering
United Kingdom
University of Huddersfield
Huddersfield, United Kingdom
<https://orcid.org/0000-0001-5992-5348>

³Karl Walton
School of Computing and Engineering
United Kingdom
University of Huddersfield
Huddersfield, United Kingdom
<https://orcid.org/0000-0002-1473-6604>

Abstract— This research is focused on exploring the utilization of Acoustic Emission (AE) in the condition monitoring of safety-critical engineering structures. AE serves as a non-destructive testing method that identifies defects and structural changes by analyzing the release of elastic energy during the initiation and progression of cracks. The proposed methodology revolves around the strategic placement of AE sensors on structures, continuous data acquisition during operational phases, and the application of advanced signal processing and pattern recognition techniques for the detection of faults and assessment of their severity. The incorporation of machine learning techniques enhances accuracy and facilitates real-time decision-making for proactive maintenance, ultimately ensuring the safety and reliability of infrastructure and industrial operations. The study underscores AE's pivotal role in extending the life of structures, minimizing downtime, and reducing maintenance expenses. In summary, AE-based condition monitoring presents significant potential for safeguarding critical engineering assets and advancing proactive maintenance practices.

Keywords— condition monitoring, machine learning, acoustic emission, signal processing, composites

I. INTRODUCTION

Composites serve as widely favoured lightweight construction materials in safety-critical engineering sectors, including aeronautics, aerospace, and automotive industries. Their appeal is attributed to several key characteristics, such as excellent resistance to water and moisture, acoustic insulation, fire resistance, a high stiffness-to-weight ratio, adaptability in construction, and robust load-bearing capabilities [1-2]. However, despite these merits, composite structures are susceptible to various forms of damage, such as fatigue cracking, indentation, debonding, and matrix failure, among others. These defects can precipitate unexpected structural failures [2-3]. Therefore, it is imperative to establish an online structural condition monitoring strategy to effectively detect concealed damage.

One promising approach for this purpose involves acoustic emission (AE), a method that involves the detection of transient elastic waves generated during damage initiation in a material. These AE waves are a result of the rapid release of energy associated with irreversible structural changes within the material [4-6]. Often, a pencil lead break (PLB) signal is employed as an AE source, offering a reproducible test signal for AE applications. Different functions, including step functions, linear functions, and cosine bell functions, have been explored for modeling the rise times of PLB signals. It has been found that the cosine bell function yields the best agreement between simulation and analytical results [8].

AE-based monitoring techniques offer the potential for large-scale, in-service monitoring with minimal instrumentation requirements. These techniques capture the elastic wave motion following the initiation and propagation of cracks within materials and convert it into electrical waveforms. Analysing these waveforms aids in understanding the nature and extent of structural damage. Remarkably, this monitoring technique enables global structural assessment and is passive in nature, drawing its energy solely from the damage source without requiring external energy sources [5-6].

In contemporary research, there is a growing emphasis on developing automated monitoring techniques that employ experimentally measured structural responses [9-11]. Among these techniques, image-based condition monitoring has emerged as a promising avenue for rapid inspection [12-14]. However, the identification of structural damage using measured data has proven to be intricate due to the influence of predefined damage features on the identification results. To mitigate this complexity, deep learning-based image classification techniques are being adopted. These techniques train neural networks using the features of the training dataset, offering an advantage in handling grid-like inputs such as images and producing consistent feature values from local regions with similar patterns. The applications of deep learning in condition monitoring encompass a wide range, including identifying cracks in concrete, road defects, pavement distress, and historical structure damage, among others [18-20].

A review of existing literature reveals a significant research gap in the domain of AE-based deep learning for the automatic detection and classification of damage sources in safety-critical composite structures, a gap that this paper seeks to address. This paper introduces a Random Forest Classifier (RFC) based deep learning model for autonomous damage source zone monitoring in sandwich composite (SCS) structures, utilizing AE signals induced by PLBs at 45° angle (approximately). A series of laboratory experiments has been conducted on a SCS using two piezoelectric AE sensors. The AE signals acquired during these experiments (in the time domain) are transformed into time-frequency RGB (red-green-blue) spectrogram through continuous wavelet transform (CWT). These spectrogram images serve as inputs for the specifically designed RFC based deep learning model for training/validation and testing.

II. LABORATORY EXPERIMENTS FOR AE BASED INSPECTION OF THE COMPOSITE STRUCTURE

A comprehensive experimental investigation was conducted on an unblemished SCS (500 mm × 500 mm × 15 mm) specimen utilizing a randomly configured network of AE

sensors. The SCS sample, composed of aluminium honeycomb core and carbon-fibre composite face-sheets, was chosen for this laboratory study. To capture sensor signals, a multi-channel acoustic data-acquisition system (ADAS) was employed.

Within the experiment, damage-induced AE-waves were generated by employing a pencil-lead-break source (referred to as HN-source) at various locations within the sensor network on the specimen. A comprehensive depiction of the experimental setup, encompassing both the ADAS system and the sensor network on the SCS sample with an existing debond region, is presented in Fig. 1.

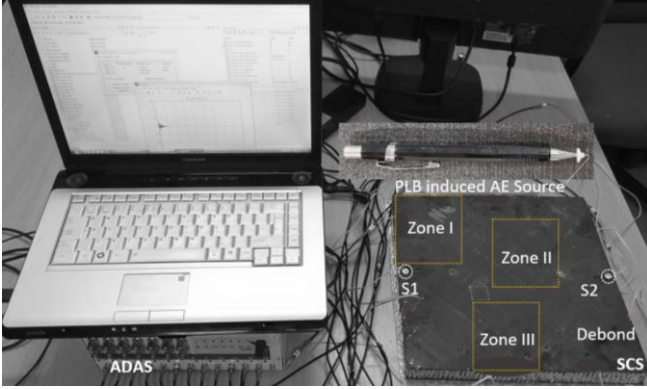


Fig. 1. Experimental setup for PLB-induced AE-based inspection of SCS.

III. DEEP LEARNING BASED AUTONOMOUS CONDITION MONITORING OF SCS

An autonomous condition monitoring strategy is developed for the rapid localization of the artificial damage sources within the three distinct zones: 'Zone I', 'Zone II', and 'Zone III'. The proposed monitoring strategy utilizes a purposely designed Random Forest classifier based deep learning model to accomplish this intelligent monitoring using the AE data registered at the pre-assigned sensing points (i.e., S1 and S2).

The initial phase entails data preprocessing, where the spectrogram images are produced by performing CWT on the received AE signals corresponding to the three different categories and standardized them to a uniform size of 136×136 pixels. These spectrograms underwent conversion into numerical arrays. The dataset was partitioned into training, validation, and test sets, with the training and validation subsets serving as the foundation for model development and the test set as an independent evaluation dataset. The Random Forest model was instantiated with 100 decision trees and subsequently underwent training utilizing the training data. During this training process, the model acquired the ability to discern and interpret the patterns inherent in the images, enabling it to detect / classify the AE source on the SCS.

Subsequent to the model's training phase, we assessed its performance on both the validation and test datasets. Predictions were made on the validation data, and the accuracy of these predictions was gauged and recorded as the validation accuracy (VA) as given in Eq. 1. Following this, predictions were generated for the test dataset, and the test accuracy (TA) as represented in Eq. 2 was ascertained.

$$VA = \frac{\text{Number of Correct Predictions on Validation Set}}{\text{Total Number of Validation Samples}} \quad (1)$$

$$TA = \frac{\text{Number of Correct Predictions on Test Set}}{\text{Total Number of Test Samples}} \quad (2)$$

To gain insights into the reliability of the model's predictions, the standard error is computed as represented in Eq. 3, a metric that quantifies the deviation of predicted labels from the true labels in the test dataset. In addition, the standard errors are estimated for each specific class ('Zone I', 'Zone II', and 'Zone III') to assess prediction variability for individual categories. An average standard error as given in Eq. 4 was derived to furnish a comprehensive measure of prediction reliability.

$$\text{Standard Error} = \sqrt{\frac{\sum_{i=1}^N (y_{\text{test-predict}} - y_{\text{test}})^2}{N}} \quad (3)$$

$$\text{Average Standard Error} = \frac{1}{N'} \sum_{i=1}^{N'} \text{Class Standard Error}_i \quad (4)$$

To extend our understanding of the model's performance, a confusion matrix is constructed. This matrix illuminates the number of true positives, true negatives, false positives, and false negatives, affording a more detailed analysis of classification accuracy. In summation, the proposed methodology performs data preprocessing, model selection, training, validation, and evaluation, standard error analysis with equations, and the construction of a confusion matrix. These integral components together constitute our approach for classifying the damage induced AE source regions, which is presented in the following section.

IV. RESULT AND DISCUSSION

The proposed condition monitoring approach leverages the Random Forest classifier based deep learning to achieve autonomous detection and classification of damage-source regions in the SCS. Towards this, a series of PLB induced AE experiments is performed in 3 predefined damage zones on the SCS. The corresponding AE signals in time-domain are collected and processed to produce spectrogram images. A typical comparison of the raw S1 signals corresponding to the Zone I, Zone II and Zone III is presented in Fig. 2.

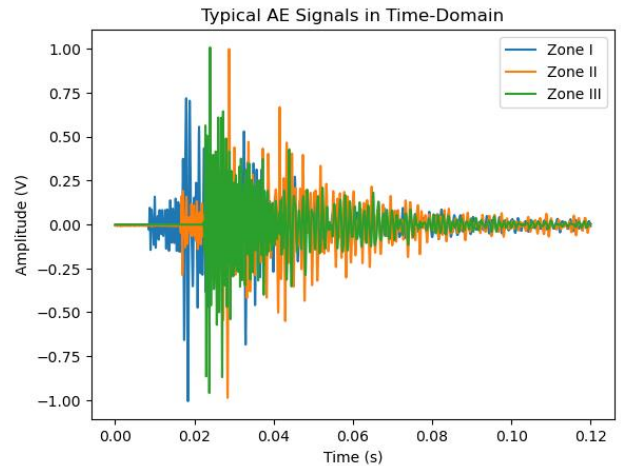


Fig. 2. AE signals corresponding to three different damage-source zones.

The time-domain AE signals are then converted to time-frequency spectrogram images as represented in Fig. 3. These spectrogram data are applied to a purposely designed deep learning model. A detailed distribution of the training, validation, testing image data corresponding to the predefined Zone I, Zone II and Zone III are listed in Table 1.

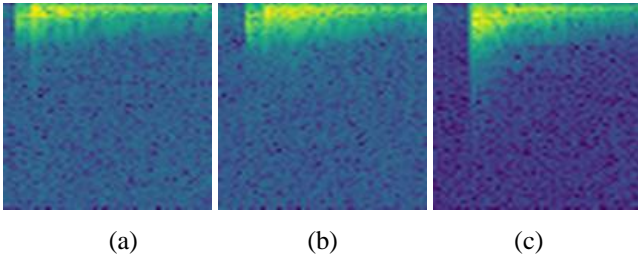


Fig. 3. CWT spectrograms of the AE signals at S1 (ref. Fig. 2) from (a) Zone I, (b) Zone II, and (c) Zone III.

TABLE I. DISTRIBUTION OF THE CWT SPECTROGRAM DATA

Condition	Table Column Head		
	Training	Validation	Testing
Zone I	1000	200	200
Zone II	1000	200	200
Zone III	1000	200	200

The training and validation performance of the proposed deep learning model is presented in Fig. 4. The proposed model offers around 97% of training accuracy and around 95% validation accuracy (95.67%) using the spectrogram data from 3 different classes (ref. Table 1). The model renders standard errors for each class are: [0.542125446737192, 0.31268994227509145, 0.3411744421846396] with an average standard error of 0.39866327706564103. In addition, Fig. 5 shows the class wise distribution of the standard error versus the average standard error for a better representation of the monitoring performance.

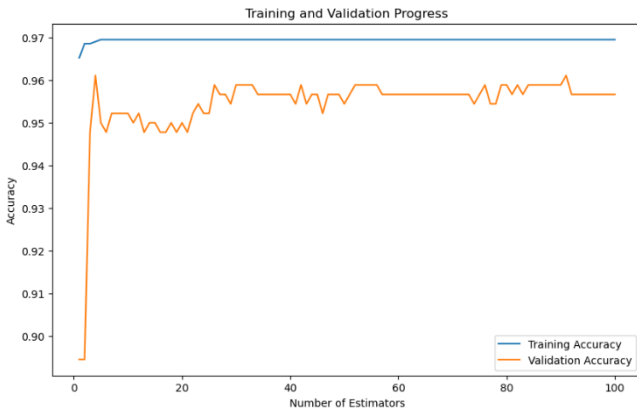


Fig. 4. Training/validation progress achieved from the deep learning model.



Fig. 5. Class wise distribution of standard error versus av. standard errors.

The test confusion matrix from the trained deep learning model is presented in Fig. 6. It shows the class-wise identification of the supplied test data per classes (i.e., 200). The model produced an average test accuracy of 91.5 % and Fig. 7 shows the class-wise test accuracy with respect to the overall (3 class average) test accuracy.

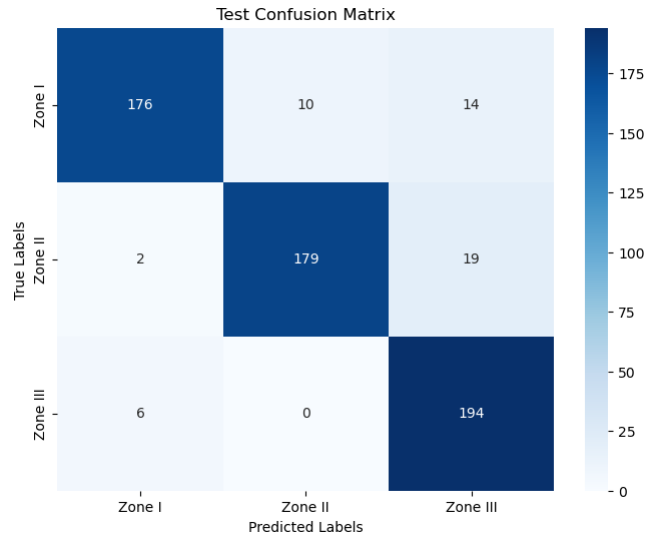


Fig. 6. Confusion matrix shows the test performance of the deep learning model for identifying the AE source regions on the SCS.

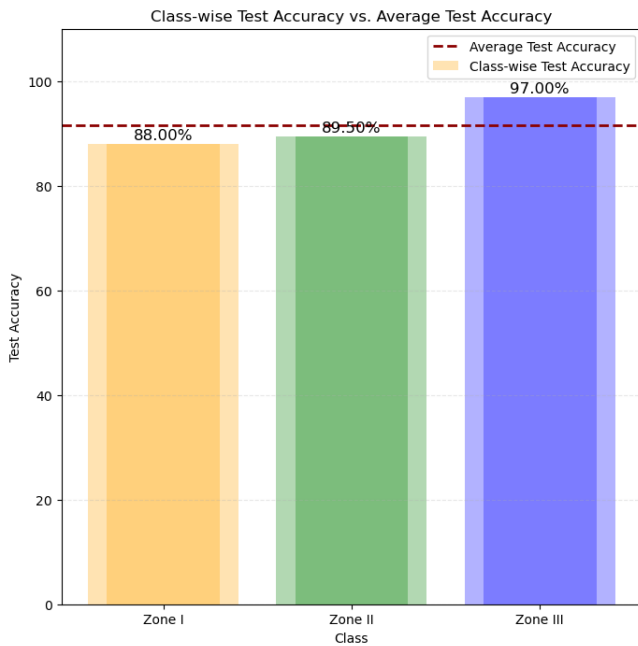


Fig. 1. The class-wise test accuracy versus the overall test performance.

V. CONCLUSION

A novel AE-based deep learning model has been introduced for the automated monitoring of damage-source regions within the SCS. This model has demonstrated remarkable efficacy in the detection of damage sources and the identification of specific zones within the targeted SCS. Notably, this Structural Health Monitoring (SHM) approach eliminates the need for intensive manual feature engineering by working directly with raw, unprocessed AE signals for comprehensive assessments of both global and localized damage sources in composite materials.

The confusion charts generated during testing of the pre-trained deep learning model underscore its capacity to reliably differentiate among the three primary AE-source regions or classes within the SCS. This high level of accuracy has been achieved using previously unused datasets, emphasizing the robustness and practical applicability of the proposed condition monitoring approach.

This research holds promise for making substantial contributions to the field of Structural Health Monitoring. It paves the way for the development of cyber-physical systems tailored for industrial-grade condition monitoring of safety-critical composite structures and systems. Looking ahead, our future research endeavours will delve into the characterization of diverse types of damage sources within operational composites, an ongoing area of investigation for the authors.

ACKNOWLEDGMENT

The research conducted in this paper has been supported by the University of Huddersfield's QR fund and the URF grant, granted under Agreement No. EEE900-10. Shirsendu Sikdar wishes to acknowledge the support from the IMP PAN Poland and Polish National Science Centre (NCN), Poland for the OPUS15 grant: UMO-2018/29/B/ST8/02904.

REFERENCES

- [1] S.T. Peters (Ed.), *Handbook of Composites*, Springer Science & Business Media, 2013.
- [2] S. Sikdar and S. Banerjee, *Structural Health Monitoring of Advanced Composites Using Guided Waves*, LAP LAMBERT Academic Publishing, 2017; ISBN 978-620-2-02697-0.
- [3] W.H. Prosser, *Advanced AE Techniques in Composite Materials Research*, *Journal of Acoustic Emission*, 1996; 14:1–11.
- [4] M. Wevers, *Listening to the Sound of Materials: Acoustic Emission for the Analysis of Material Behavior*, *NDT&E Int*, 1997; 30:99–106.
- [5] M. Wevers and K. Lambrighs, *Applications of Acoustic Emission for SHM: A Review*, *Encyclopedia of Structural Health Monitoring*, John Wiley & Sons, 2009.
- [6] K. Ono and A. Gallego, *Research and Application of AE on Advanced Composite*, *Journal of Acoustic Emission*, 2012; 30:180–229.
- [7] K.R. Miller and E.K. Hill, *Non-Destructive Testing Handbook, Acoustic Emission Testing*, American Society for Non-Destructive Testing, 2005.
- [8] M.G. Sause, *Investigation of Pencil-Lead Breaks as Acoustic Emission Sources*, *Journal of Acoustic Emission*, 2011; 29.
- [9] F. Liu, S. Gao, Z. Tian, and D. Liu, *A New Time-Frequency Analysis Method Based on Single Mode Function Decomposition for Offshore Wind Turbines*, *Marine Structures*, 2020; 72:102782.
- [10] H. Liu and Y. Zhang, *Image-Driven Structural Steel Damage Condition Assessment Method Using Deep Learning Algorithm*, *Measurement*, 2019; 133:168-81.
- [11] S. Sikdar, D. Liu, and A. Kundu, *Acoustic Emission Data-Based Deep Learning Approach for Classification and Detection of Damage-Sources in a Composite Panel*, *Composites Part B: Engineering*, 2022; 228:109450.
- [12] Y. Jia, E. Shelhamer, J. Donahue, S. Karayev, J. Long, R. Girshick, S. Guadarrama, and T. Darrell, *Caffe: Convolutional Architecture for Fast Feature Embedding*, In *Proceedings of the 22nd ACM International Conference on Multimedia*, 2014 Nov 3; pp. 675–678.
- [13] S. Sikdar and J. Pal, *Bag of Visual Words-Based Machine Learning Framework for Disbond Characterization in Composite Sandwich Structures Using Guided Waves*, *Smart Materials and Structures*, 2021 May 14; 30: p. 075016.
- [14] A. Jacobsen, T. Hitaka, and M. Nakashima, *Online Test of Building Frame with Slit-Wall Dampers Capable of Condition Assessment*, *Journal of Constructional Steel Research*, 2010 Nov 1; 66(11):1320-9.
- [15] F.C. Chen and M.R. Jahanshahi, *NB-CNN: Deep Learning-Based Crack Detection Using Convolutional Neural Network and Naïve Bayes Data Fusion*, *IEEE Transactions on Industrial Electronics*, 2017 Oct 19; 65(5):4392-400.
- [16] C. Tao, C. Zhang, H. Ji, and J. Qiu, *Fatigue Damage Characterization for Composite Laminates Using Deep Learning and Laser Ultrasonic*, *Composites Part B: Engineering*, 2021 Jul 1; 216:108816.
- [17] C. Suresh Kumar, V. Arumugam, and C. Santulli, *Characterization of Indentation Damage Resistance of Hybrid Composite Laminates Using Acoustic Emission Monitoring*, *Composites Part B: Engineering*, 2017; 111:165-178.
- [18] Young-Jin Cha, Wooram Choi, and Oral Büyüköztürk, *Deep Learning-Based Crack Damage Detection Using Convolutional Neural Networks*, *Computer-Aided Civil and Infrastructure Engineering*, 2017; 32(5):361-378.
- [19] Hongbing Shang, et al., *Deep Learning-Based Borescope Image Processing for Aero-Engine Blade In-Situ Damage Detection*, *Aerospace Science and Technology*, 2022; 123:107473.
- [20] Yao Yao, Shue-Ting Ellen Tung, and Branko Glisic, *Crack Detection and Characterization Techniques—An Overview*, *Structural Control and Health Monitoring*, 2014; 21(12):1387-1413.